RAPID AND ROBUST DYNAMICS-BASED NONDESTRUCTIVE METHOD FOR AEROSPACE STRUCTURAL HEALTH MONITORING

An Air Force STTR Award for PROJECT F045-016-0125
CONTRACT NO. FA9550-04-C-0078

Final Report

Submitted To:

USAF, AFRL
AF Office of Scientific Research (AFOSR)
4015 Wilson Blvd., Rm. 713
Arlington, VA 22203-1954

By

Pizhong Qiao, Ph.D., P.E.
Integrated Smart Structures, Inc.
2601 Twin Creeks Dr., Copley, OH 44321-1770
Ph: (330) 664-0982; Email: pzqiao@gmail.com

and

Wahyu Lestari, Ph.D.
The University of Akron
Department of Civil Engineering, 244 Sumner Street, Akron, OH 44325-3905
Ph: (330) 972-5226; Email: lestari@uakron.edu

20050622 105

JUNE 14, 2005

AFRL-SR-AR-TR-05-

0228

REPORT DOCUMENTATION PAGE

1. REPORT DATE (DD-MM-YYYY)	2. REPORT TYPE	3. DATES COVERED (From - To)
14-06-2005	Final Technical Report	15 Aug 2004 - 14 Jun 2005

4. TITLE AND SUBTITLE	5a. CONTRACT NUMBER
Rapid and Robust Dynamics-based Nondestructive Method for Aerospace Structural Health Monitoring	FA9550-04-C-0078
	5b. GRANT NUMBER
	5c. PROGRAM ELEMENT NUMBER

6. AUTHOR(S)	5d. PROJECT NUMBER
Qiao, Pizhong	
	5e. TASK NUMBER
Lestari, Wahyu	
	5f. WORK UNIT NUMBER

7. PERFORMING ORGANIZATION NAME(S) AND ADDRESS(ES)	8. PERFORMING ORGANIZATION REPORT NUMBER
Integrated Smart Structures, Inc. 2601 Twin Creeks Drive Copley, OH 44321-1770 The University of Akron Department of Civil Engineering 244 Sumner Street Akron, OH 44325-3905	ISS0004-F

9. SPONSORING / MONITORING AGENCY NAME(S) AND ADDRESS(ES)	10. SPONSOR/MONITOR'S ACRONYM(S)
USAF, AFRL AF Office of Scientific Research	AFOSR
4015 Wilson Blvd., Rm. 713 Arlington, VA 22203-1954	11. SPONSOR/MONITOR'S REPORT NUMBER(S)

12. DISTRIBUTION / AVAILABILITY STATEMENT
Approved for public release; distribution unlimited.

13. SUPPLEMENTARY NOTES
None

14. ABSTRACT

Report developed under STTR contract for Topic F045-016-0125 addresses dynamic-based damage identification techniques for structural health monitoring (SHM) of aerospace structures. Two systems (i.e., the scanning laser vibrometer (SLV) and PVDF sensor) are used to acquire the dynamic information, and effective damage detection algorithms (e.g., the gapped smoothing method (GSM) and generalized fractal dimension (GFD)) and schemes (e.g., the uniform load surface (ULS) and combined static/dynamic techniques) are developed to evaluate the damage. It is demonstrated that both the GSM and GFD methods are capable of identifying damage without baseline information of healthy structure. Application of the static/dynamic approach improves the performance of the damage identification, and the ULS increases the effectiveness of the detection at low modes. In general, the PVDF sensor system is good for acquiring several low curvature mode shapes; while the SLV system can generate higher displacement modes. Utilizing the advantages of each measurement system, the proposed identification algorithms have great potential for viable SHM products, e.g., the PVDF sensor system for on-board and the SLV system for portable on-site monitoring. The proposed sensor systems and developed identification techniques pave the foundation for further refinement of the dynamics-based method, field implementation and commercial product development.

15. SUBJECT TERMS
STTR Report; Aircrafts; Plates; Damage Detection; PVDF Sensors; Scanning Laser Vibrometer; Dynamics

16. SECURITY CLASSIFICATION OF:			17. LIMITATION OF ABSTRACT	18. NUMBER OF PAGES	19a. NAME OF RESPONSIBLE PERSON
a. REPORT U	b. ABSTRACT U	c. THIS PAGE U	SAR		Qiao, Pizhong
					19b. TELEPHONE NUMBER (include area code) (330)972-5226

6-21-05

Table of Contents

1 INTRODUCTION

1.1 Identification and Strategic Significance of the Problem

Structural health monitoring (SHM) is one of the most important tools to maintain safety and integrity of aerospace structural systems. Early detection or monitoring is the key part of structural preventive maintenance program, which ensures the safety and integrity and ultimately enhances the life of structures and the affordability of structural system. Hence, a robust and reliable nondestructive damage identification and assessment is essential for the development of such monitoring systems.

The objective of this STTR Phase I project is to develop a dynamics-based identification procedure for health monitoring systems. The ultimate goal of SHM technology is to develop autonomous systems for continuous monitoring, inspection and damage detection of structures with minimum labor involvement [1]. The monitoring system will regularly acquire and analyze the response data, preferably while the structure is in service, and indicate the damage, as graphically illustrated in Figure 1. Dynamic responses, which may be obtained by a surface measurement, provide useful information about the structural health without costly dismantling procedures of the structures. Changes in the dynamic characteristics can be related to the changes of the structural physical properties and used to locate and assess damages. Several researches on structural and mechanical system health monitoring based on dynamic characteristic changes were reported by Doebling et al. [2].

Information of the structural conditions immensely depends on the measurement of data. Hence the method of acquiring data must be reliable and robust, and the placement of sensors and measurement system should have minimum interference to the function of the structure. In addition, from the philosophy of SHM, the process of acquiring data should be user-friendly and involve minimum labor. Number of sensors distributed in the structure, attachment method of sensors, and total weight of the system are some of the significant issues in implementation of the detection method in actual testing conditions, which need to be addressed. Under certain limitations in field, which may result in limited number of measurement locations, the technique should perform well.
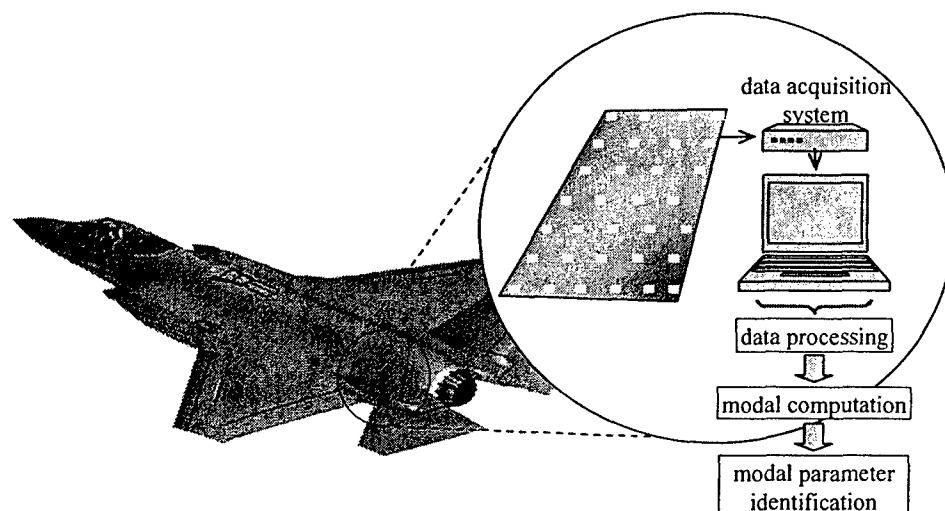

Figure 1 Structural health monitoring for aerospace systems, with on-board data acquisition system

1.2 Technical Objectives

The purpose of this collaboration between Integrated Smart Structures, Inc. (ISSI) and the University of Akron (UA) in the STTR program is to develop an effective and robust nondestructive damage identification technique using dynamic response information, which eventually evolves to a portable device system for on-site structural health monitoring applications, with particular emphasis on monitoring of aerospace structures. Using a combined experimental and analytical/numerical approach, a rapid and robust dynamics-based damage detection technique with aid of smart piezoelectric sensors and actuators and scanning laser vibrometer (SLV) is developed. The following technical goals are accomplished in this STTR project:

1.   Development of damage identification algorithms,

2.   Sensor systems selection,

3.   Analytical/numerical simulation,

4.   Data processing,

5.   Experimental demonstration.

In this final report, the works and results of the above activities are described and illustrated. The challenges to minimize prior data or model dependencies and to account for the constraints in the field implementation of the technique are addressed as well.

2   DAMAGE IDENTIFICATION APPROACH

Several damage identification algorithms based on dynamic responses are proposed and evaluated. Both the displacement/curvature mode shapes and natural frequency are considered in the dynamic analysis. Although, the presence of damage can be easily recognized by observing changing in natural frequency of the structures, locating damage and quantifying its extent need much more complex procedure. In this study, some newly developed algorithms (e.g., the generalized fractal dimension (GFD) and combined static-dynamic techniques) and the existing effective and unique approaches (e.g., the gapped smoothing and the uniformed load surface (ULS) methods) are introduced, and their theoretical backgrounds are briefly described as follows.

2.1 Generalized Fractal Dimension (GFD)

The concept of fractal and its corresponding mathematical properties were established by French mathematician Mandelbrot [6]. In measuring a fractal curve, if we reduce the ruler length by $1/r$, its length would correspondingly increase to $L = r^D$ multiplying the original one. D is called the fractal dimension (FD) of a fractal curve. A regular smooth curve has a dimension of 1; while a fractal curve has a fraction dimension which is greater than 1. In general, the larger the value of D, the more irregular the curve does. Therefore, the fractal dimension has a potential to serve as a damage detector revealing the irregularity introduced by a local damage in a structure as demonstrated in a recent study by using the Katz's Fractal Dimension (FD) expression [7]

$$FD_M(x) = \frac{\log(n)}{\log(n) + \log\left(\frac{d(x_i, M)}{L(x_i, M)}\right)} \tag{1a}$$

$$L(x_i, M) = \sum_{j=1}^{M} \sqrt{\left(y(x_{i+j}) - y(x_{i+j-1})\right)^2 + \left(x_{i+j} - x_{i+j-1}\right)^2} \tag{1b}$$

$$d(x_i, M) = \sum_{1 \le j \le M}^{M} \sqrt{\left(y(x_{i+j}) - y(x_i)\right)^2 + \left(x_{i+j} - x_i\right)^2} \tag{1c}$$

where $x = \frac{1}{2}(x_i + x_{i+M})$, $n = L/\overline{\alpha}$ and $\overline{\alpha}$ is the average distance between successive points. M is the sliding window sampling length, and $M = 4$ is chosen in this study [8].

However, in certain damage configuration such as the location of damage in the vicinity of maximum point of the deformation, the FD-based detection method resulted in a misleading information. A modified FD is developed by the investigators [8] to overcome this shortcoming of the FD damage detection technique. Inspired by the wavelet transformation, a scale parameter S is introduced in the FD expression and the modified FD is denoted as a generalized fractal dimension (GFD). By changing the S value, the resulting GFD has a multi-scale feature and is defined as

$$GFD_{M,s}(x) = \frac{\log(n)}{\log(n) + \log\left(\dfrac{d_S(x_i, M)}{L_S(x_i, M)}\right)} \tag{2a}$$

$$d_S(x_i, M) = \max_{1 < j \le M} \sqrt{\left(y(x_{i+j}) - y(x_i)\right)^2 + S^2\left(x_{i+j} - x_i\right)^2} \tag{2b}$$

$$L_S(x_i, M) = \sum_{j=1}^{M} \sqrt{\left(y(x_{i+j}) - y(x_{i+j-1})\right)^2 + S^2\left(x_{i+j} - x_{i+j-1}\right)^2} \tag{2c}$$

Noting that by changing the S value, the resulting GFD has a multi-scale feature. Compared with the mode shape itself, the irregularity caused by the damage on the deformation shape is local, and we can therefore filter the peak value of FD introduced by the mode shape itself while keeping the one caused by the local damage through choosing a proper scale value S. Since the GFD bears no conventional physical meaning as compared to the FD, it only serves as an indicator of damage in this study. Detail description of the GFD based-damage identification approach can be seen in the paper by Wang and Qiao [8].

2.2 Uniform Loading Surface (ULS)

Flexibility, which contains the internal force distribution due to external loading and support conditions, is a significant source of information regarding the structural condition. Using modal space parameters, the flexibility can be well approximated and used for structural identification. The modal flexibility is not exactly the static flexibility; it is the accumulation of the modal vectors contribution to the flexibility. The modal flexibility is relatively insensitive to data truncation and boundary conditions. Therefore, the modal flexibility can be well defined by using limited modal vectors identified experimentally.

For a structural system with n degrees-of-freedom, the modal flexibility matrix is given by the following expression [9]

$$F = \sum_{r=1}^{n} \frac{\phi_r \phi_r^T}{\omega_r^2} \tag{4}$$

where ϕ_r is the rth normalized mode shape and ω_r is the corresponding r^{th} natural frequency. In practice, the modal testing can only yield several low modes. With m modes available from experimental data, the modal flexibility matrix of the structure can be approximated as

$$F = [f_{i,j}] = \sum_{r=1}^{m} \frac{\phi_r \phi_r^T(j)}{\omega_r^2} \qquad (5)$$

in which $f_{i,j}$ describes the modal flexibility at the ith point under the unit load at the point j and is the summation of the product of the related term from available modes. Hence, the displacement vector can be obtained by multiplying the flexibility matrix with the loading vector. When all degrees of freedom are subjected to a unit load together, the resulting displacement vector is called the uniform load surface (ULS). It is difficult to achieve this condition in actual structure, assuming that a linear system approximation of the mode shape under uniform loading based on the flexibility matrix is valid. For a structural system with m mode shapes data and n degrees of freedom, the deflection vector U of the structure under uniform load (ULS) can be defined as

$$U = [f_{i,j}]\{l_j\} = \begin{bmatrix} f_{1,1} & f_{1,2} & \cdots & f_{1,n} \\ f_{2,1} & f_{2,2} & \cdots & f_{2,n} \\ \vdots & \vdots & \vdots & \vdots \\ f_{n,1} & f_{n,2} & \cdots & f_{n,n} \end{bmatrix} \begin{Bmatrix} 1 \\ 1 \\ \vdots \\ 1 \end{Bmatrix} \qquad (6)$$

with

$$u(i) = \sum_{j=1}^{n} f_{i,j} = \sum_{r=1}^{m} \frac{\phi_r(i)}{\omega_r^2} \sum_{j=1}^{n} \phi_r(j) \qquad (7)$$

or

$$U = F \cdot L \qquad (8)$$

where F is the modal flexibility matrix and $L = \{1, \cdots, 1\}_{1 \times n}^T$ is the unit vector representing the uniform load acting on the structure. Each term in the summation for deflection vector $u(i)$ has the corresponding frequency in the denominator, and this results in rapid decrease of the higher mode term contribution. Hence, the ULS can be well approximated by only a few lower mode terms. Because the technique considering the ULS reduces the sensitivity of the damage identification to the mode shape choices, it is adapted in this study to evaluate the location and relative magnitude of damage.

2.3 Gapped Smoothing Method (GSM)

In some cases such as structures that are already in service for long period, data of healthy or undamaged structures are rarely available. These data can be approximated by using a gapped-smoothing technique, where the basic assumption of the technique is that a mode shape of a healthy structure has a smooth surface [10]. Using the mode shape data of damaged structure and interpolation technique with polynomial approximation, the smooth mode shape surfaces of healthy structure are estimated. In this research, the technique is modified by assuming one polynomial expression for the entire deflection, instead of calculating one segment at a time. The modified technique reduces the calculation time for the estimation process. For the plate structures, the undamaged deflection is approximated by using a polynomial in two variables as follows

$$U_{GSM}(x,y) = \sum_{i=0}^{n}\sum_{j=0}^{m} C_{ij}X^iY^j \tag{9}$$

where the C_{ij} is the coefficients calculated by using surface-fitting. The Damage Index (DI) based on this approach is calculated as the square of the difference between the measured data of the damaged structure, U_d, and the fitted value represented the healthy data, U_{GSM}

$$DI(x,y) = (U_d(x,y) - U_{GSM}(x,y))^2 \tag{10}$$

2.4 Combined Static-dynamic Technique

The purpose of the combined static-dynamic technique allows us to perform detection algorithm without having the data of healthy structure. The proposed technique uses reference data from measurement of unloaded structures, instead of using the originally healthy data, which is not always available. The statically loaded structure is used to make damage more pronounced, such as to make cracks or delaminations open, which results in more distinctive dynamic responses, and considered as the "damaged" structures. Different damage may behave differently under certain loading conditions, either open or close. Comparisons of the modal parameters at different static loading conditions are used to identify damage in this study.

Several loading conditions are applied to the structures, and the effectiveness of the technique is evaluated. The loading should be large enough to make a difference between the open and close conditions of damage. For the delamination, the compression loading will enhance the opening and closing cycle. On the other hand, the matrix crack opening will increase in a tension loading condition. First, the numerical parametric study on the magnitude of applied static load is conducted, for both the tension and compression loading up to about twenty percent of ultimate load of the structures. Then, the results of this study are implemented in the experimental demonstration, where the loading are applied mechanically.

3 SENSOR SYSTEMS

Two measurement systems are used and evaluated in this project, i.e., scanning laser vibrometer (SLV) system (Figure 2) and polyvinylidene floride (PVDF) sensors system (Figure 3). The scanning laser vibrometer (SLV) (Figure 2) is a non-contact system that can be considered as a distributed sensor system, since it can scan and measure the dynamic response at large number of spatial points on a structure. The SLV measurement generates many displacement modal shapes effortlessly and without worrying about sensor attachment and wiring system problem. Complemented with programmable electronic devices or chips to process the data and compute the damage parameters, this technology has great potential for development of portable on-site monitoring system.
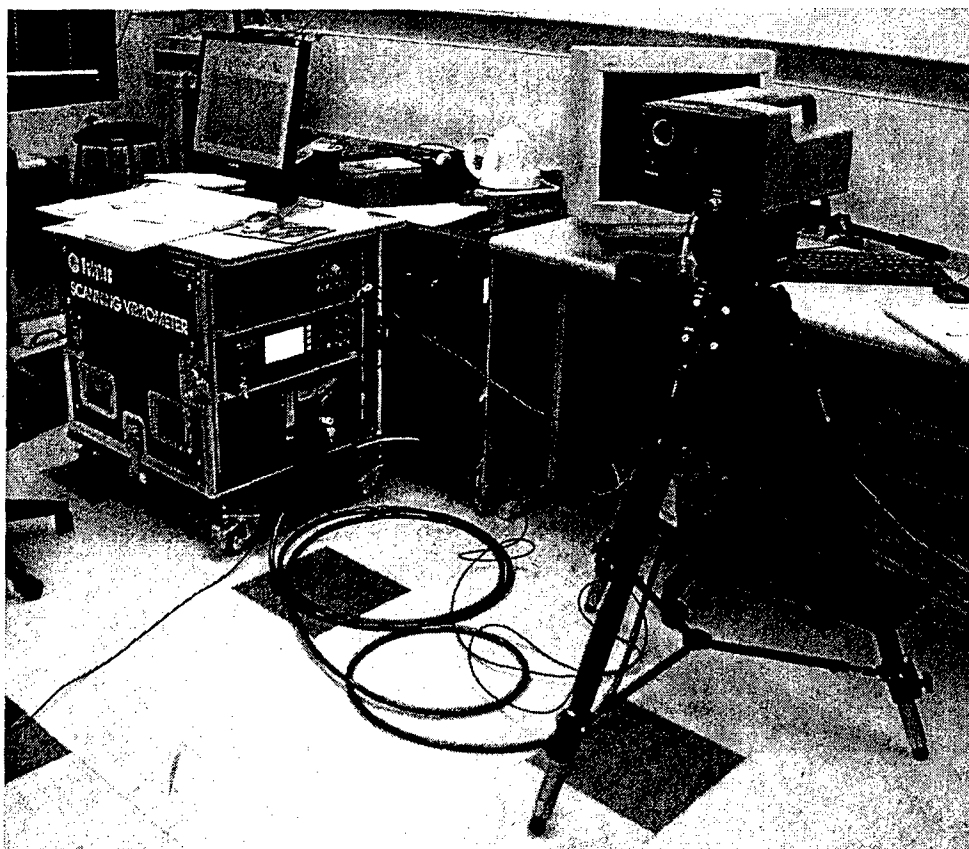
**Figure 2 Scanning Laser Vibrometer (SLV) system**

On the other side, the piezoelectric materials need to be carefully incorporated to the structure to form a diagnostic sensor system, as the quality of the interface between the host structure and sensors will also affect the measurement. Moreover, these sensors are sensitive to electric interference as well. However, this type of sensors (such as the PVDF sensors used in this study, see Figure 3(b)) measures the curvature of the structure directly, which simplify the computational procedure. Further, the curvature mode shape is more sensitive to local bending stiffness changes compared to the displacement mode shape obtained from the SLV system. Location of the sensors will be arranged with the aid of the results from numerical simulation discussed in Section 4.

For a large array of sensors, additional electronic circuitry can be developed to neatly organize the sensor wiring and data transfer. The PVDF sensor system has huge potential for development of an on-board automated monitoring system and possible integration with wireless communication technologies (e.g., integrating with the MEMS chips developed by the New Jersey Microsystems, Inc. – one of the ISSI's strategic partners).

Measured data from both the systems are post-processed and analyzed to generate the modal parameters, i.e., natural frequencies and mode shapes. Performances of each sensor system in generating data for damage identification are evaluated. Both the sensor systems have great potential for structural monitoring system, where their appropriate applications define their advantage characteristics as well as the shortcoming.
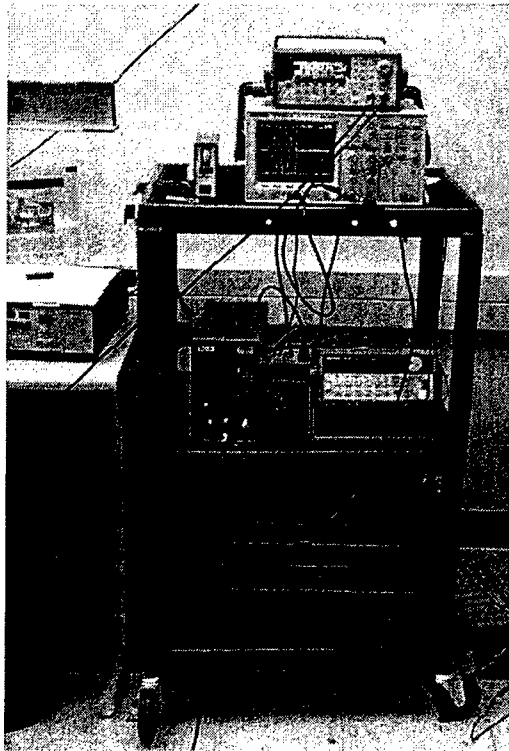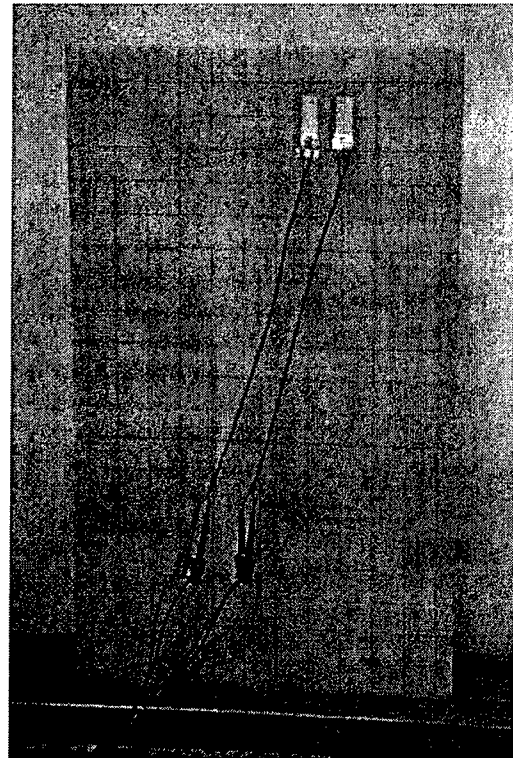
(a) Data acquisition system   (b) PVDF sensors

Figure 3 PVDF sensors system

4 NUMERICAL SIMULATION

The dynamic behavior of the panels that have various types of damage, boundary and loading (e.g., the aforementioned combined static-dynamic technique) conditions are evaluated by using the numerical simulation. The numerical results are also served as a validation tool to guide experimental work and provide insight on the physical response caused by the damage. The numerical models targeted primarily for damage simulation are developed to generate reference data and illustrate the changes in the structural response due to damage.

The numerical simulation is carried out by using commercial finite element analysis software ANSYS. The aluminum panel is modeled with Solid45 element; while the composite panels are modeled with layered element Solid46. Crack type of damage in the aluminum panel is modeled by introducing two nodes at the same grid points of the damage location. These nodes are unconnected and act independently during vibration analysis. The delaminations in the composite panels are modeled by using bilinear spring elements Link10, where these spring link elements have a unique feature of a bilinear stiffness matrix that can be set in a tension-only or compression-only element. The delaminations are modeled by compression-only link elements connecting the nodes at both sides of the delaminations. These elements have the stiffness equal to the through-the-thickness stiffness of the composite materials when in the compression state, while the stiffness goes to zero in the tension state. The compression and tension states represent the close and open conditions of the delamination during vibration, respectively. The material properties used in the FE simulations of aluminum and composite plates are given in Table 1.

The natural frequencies resulted from the FE analysis are presented in Tables 2 and 3, for the aluminum panels (Aluminum-Cantilever-Healthy: **Alu-CL-H**; Aluminum-Cantilever-Saw cut Damage: **Alu-CL-SD**) and the clamped-clamped composite panels (Composite-Clamped-Clamped-Healthy: **Comp-CC-H**; Composite-Clamped-Clamped Edge Damage: **Comp-CC-ED**), respectively. The mode shapes of healthy and damage panels are presented in Figures 4 and 5, respectively.

Using the proposed numerical model, a parametric study is also conducted for the proposed concept of combined static-dynamic approach. Based on the parametric study, the best combination of loading condition is implemented in the demonstration test. The results are examined, and necessary adjustments to the detection algorithms are incorporated to assure the performance of the proposed technique in the actual conditions.

Table 1 Material properties of aluminum and composite plates used in the FE analysis

Material	E_x (GPa)	E_y (GPa)	G_{xy} (GPa)	G_{xz} (GPa)	v_{xy}
Aluminum	70	70	26.3	26.3	0.33
E-glass/epoxy Composite	24	4.7	2.17	2.1	0.4

Table 2 FE predicted frequencies of cantilever aluminum panels, healthy (Alu-CL-H) and with saw cut damage (Alu-CL-SD)

Mode number	Healthy (Hz)	Damaged (Hz)
1	8.16	8.06
2	29.83	30.12
3	50.7	49.32
4	99.42	101.32
5	140.34	136.45
6	161.51	154.75
7	198.56	201.26
8	231.83	230.18
9	284.52	284.16
10	337.94	339.28
11	350.80	348.56
12	418.10	405.19
13	469.38	483.56
14	484.65	492.48
15	506.56	513.84

Table 3 FE predicted frequencies of clamped-clamped composite panels, healthy (Comp-CC-H) and with edge damage (Comp-CC-ED)

| Mode number	Healthy (Hz)	Damaged (Hz)
1	58.88	58.78
2	75.92	75.02
3	159.88	159.39
4	182.01	181.97
5	209.54	208.52
6	307.24	305.29
7	314.86	313.76
8	340.82	338.92
9	434.27	431.38
10	482.37	481.84
11	489.39	487.36
12	505.46	502.39
13	546.56	540.66
14	592.36	587.14
15	624.57	618.51

Mode number	Healthy cantilever aluminum panel (Alu-CL-H)	Healthy clamped-clamped composite panel (Comp-CC-H)
1		
2		
3		
4		
5		
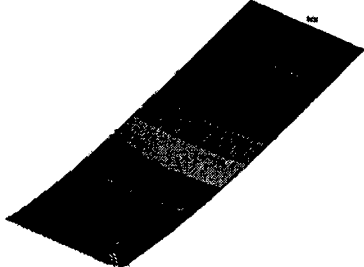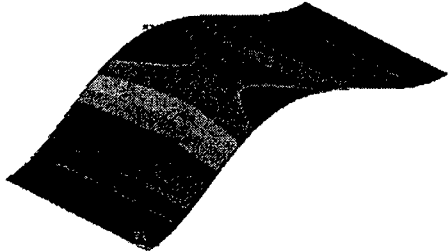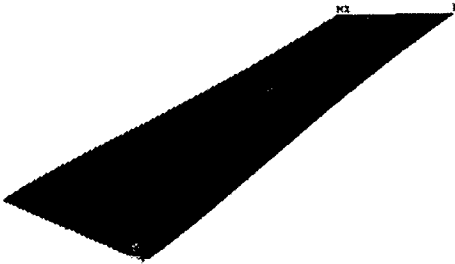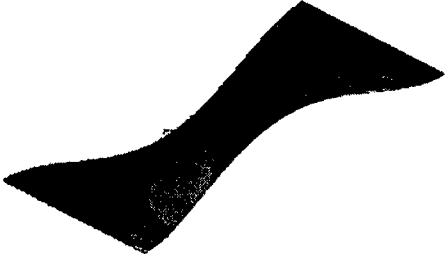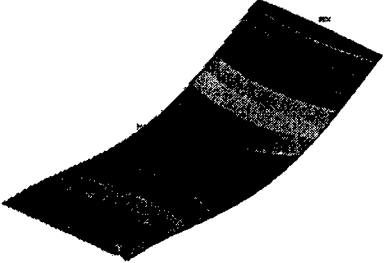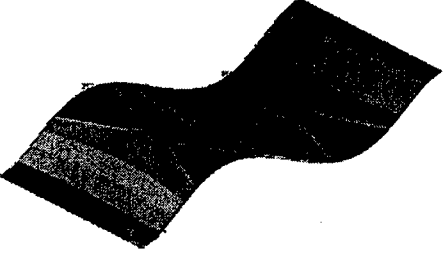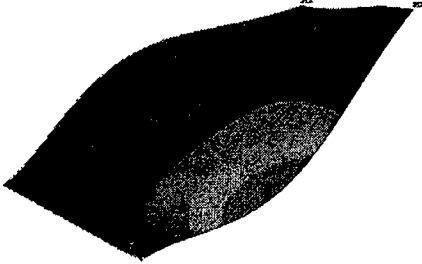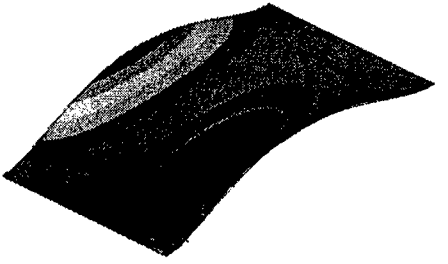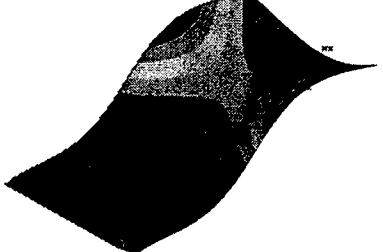
Figure 4 The first five mode shapes of healthy panels from FE model of the aluminum and composite specimens

Mode number	Aluminum panel with saw cut (Alu-CL-SD)	Composite panel with edge delamination (Comp-CC-ED)
1		
2		
3		
4		
5		
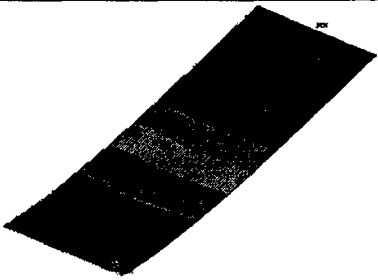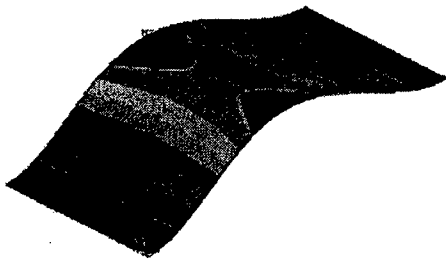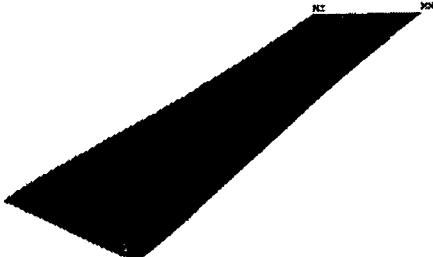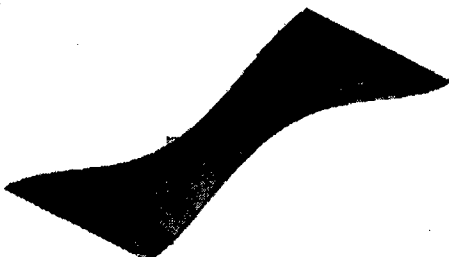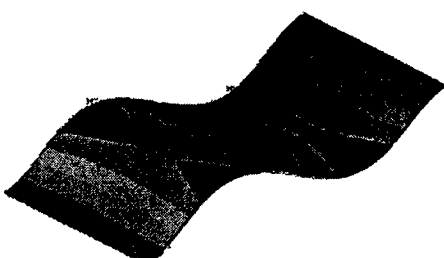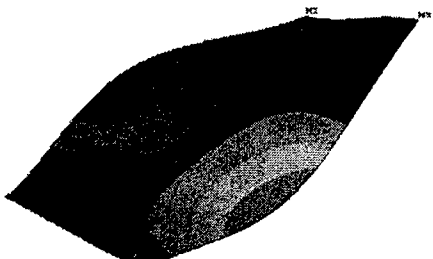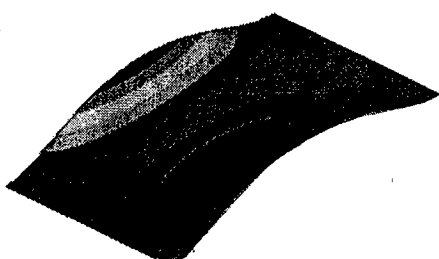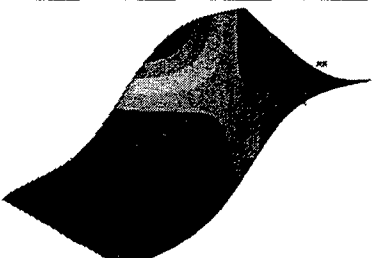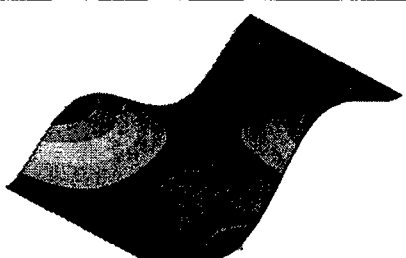
Figure 5 The first five mode shapes of damaged panels from FE model of the aluminum and composite specimens

5   DATA PROCESSING

In the data processing, two main procedures are conducted before the measured data are ready to be analyzed for damage parameters calculation. The first step is the modal analysis procedure, where the measured data are analyzed to generate the natural frequencies and mode shapes information. The second step is to obtain the unit load surface (ULS) deformation, where the mode shapes are defined as the result of uniform loading at each measurement point. This process that involves summation of the term corresponding to each measured mode reduces the sensitivity of the mode shapes to the experimental error. MATLAB and MEScope commercial programs are used to perform data transformation and processing, and modal analysis, respectively.

The two sensor systems measured and acquired different type of data. The measured data from PDVF sensors are dynamic response in the time domain; while the SLV system acquired the frequencies and mode shapes simultaneously. Hence, several steps in the data processing of each measured data are different. Data processing of the proposed structural health monitoring based on the PVDF sensor system measurement is summarized in Figure 6, and the one based on the SLV system is summarized in Figure 7.
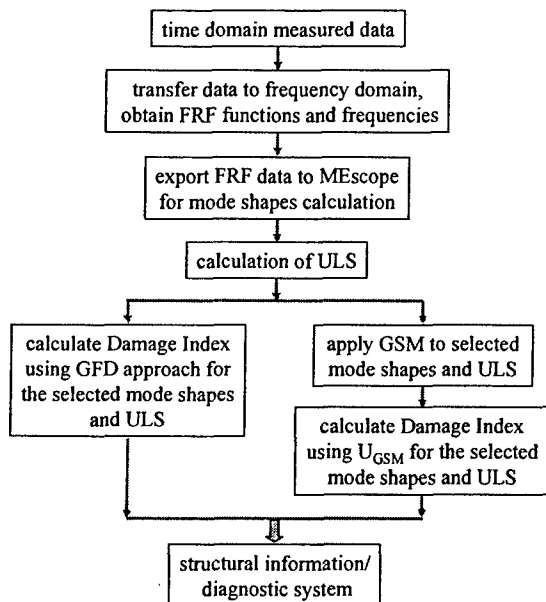

**Figure 6 Flowchart of data processing of
PVDF sensor system data**
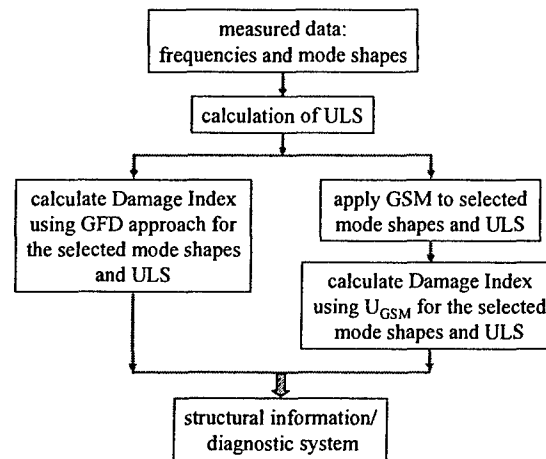
**Figure 7 Flowchart of data processing of
PVDF sensor system data**

6   EXPERIMENTAL DEMONSTRATION

Results from numerical simulation (see Section 4) are used as a guideline in conducting the experimental demonstration of the proof of concept, including number of modes necessary for damage identification, selection of mode shapes and required sampling frequency. The size of the aluminum panel is about 0.31 m ×0.56 m and the composite panel is about 0.31 m ×0.61 m, and after put in the fixtures, the panels have the same size, about 0.31 m × 0.51 m. The aluminum panels with small crack created using the fine saw-cut are prepared; while the

composite panel with edge delamination is manufactured as well. The locations and the size of damages are presented in Figure 8. To ensure a good repeatability of the experiment, a piezoelectric ceramic wafer is bonded to each panel to generate excitation. Sample of specimens are presented in Figure 9.

The composite panel is made of E-glass fiber and epoxy resins and had a [CSM/0/90/0]s lay-up for a total of eight layers, and the predicted material properties are given in Table 1. A edge delamination is created during the fabrication of the samples by inserting a piece of Teflon film between the second and the third layers. After manufacturing, some force is applied to the delamination to break it open. Again, for the sake of simplicity, the aluminum panel with a saw-cut damage is denoted as Alu-CL-SD, and the composite panel with an edge-delamination as Comp-CC-ED. These notations (i.e., Alu-CL-SD and Comp-CC-ED) are used in the rest of the report.


(a) Alu-CL-SD   (b) Comp-CC-ED
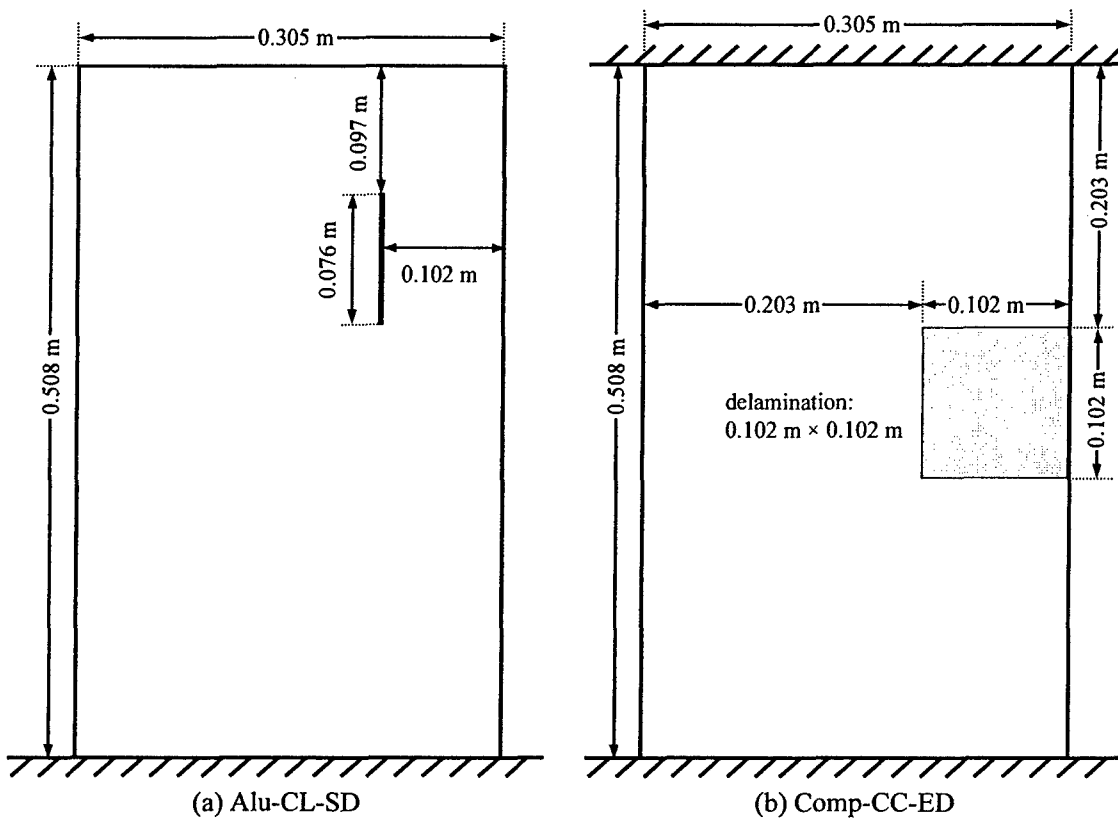
Figure 8 Specimens dimensions and damage information

(a) Alu-CL-SD   (cb) Comp-CC-ED
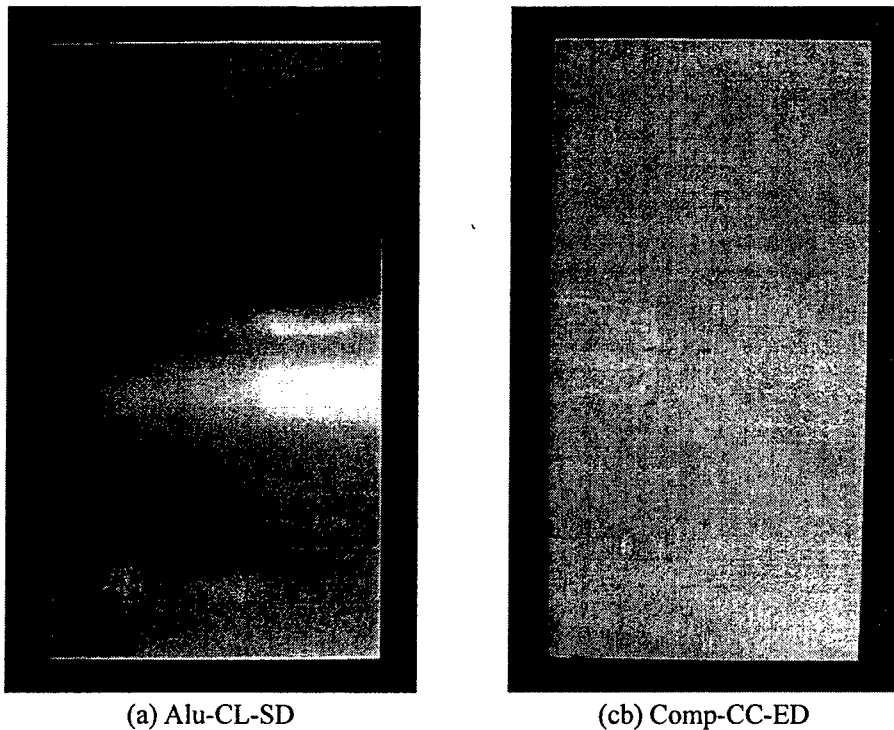
Figure 9 Sample of specimens

6.1 Experimental Set-up

For the experiment using piezoelectric sensor system, small PVDF sensors (see Figure 2) are placed on the surface of the specimen with placing arrangement suggested by the numerical finite element simulation results. The wiring is set up to provide the connection with equipment. Signals from the sensors and actuators are collected by a digital signal-processing device, which is connected with a computer for data recording. Then, the measured data are post-processed, and damage parameters are computed as described in Section 5.

For the experiment using SLV system, the scanning head of the SLV system (see Figure 3) is set up in front of the specimen to measure data at many equally spaced points on the surface of the panel. The vibrometer controller box and junction box are connected to both the scanning head and the computer. A built-in video camera system provides a composite video signal to the computer, and the image of shape of the scanned area can be stored for further data computation.

Two boundary conditions are evaluated, i.e., cantilever (CL) and clamped at both sides (CC). A fixture with sturdy steel base (Figure 10) is build to provide a cantilever condition (CL) with a stable support mounted on a heavy steel beam. The clamped-clamped condition (CC) is simulated by using an MTS machine (Figure 11), which is later also used to apply the static load. The specimen is excited with a pseudo-random signal or sweep-sine signal by a waveform signal generator, up to the frequency of interest. Several values of the static loading are evaluated and used for comparison in the damage parameters calculation. These experimental activities are primarily conducted at the University of Akron using their available laboratories and facilities.
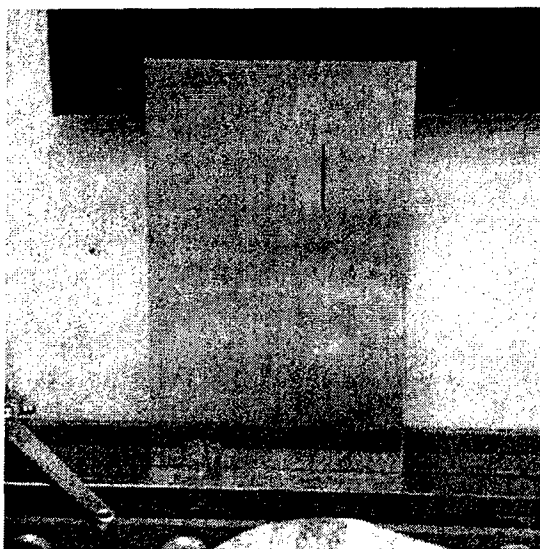
Figure 10 Aluminum plate with saw cut damage in cantilever configuration using a steel base
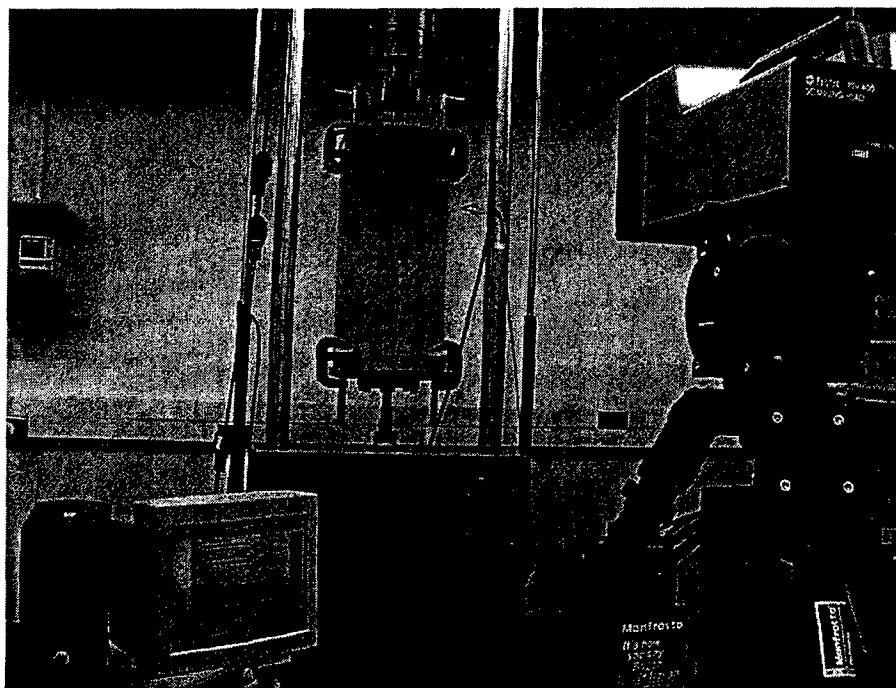

Figure 11 Experimental set-up for combined static-dynamic test

6.2 Experimental Results

The experiment data and the damage identification results from both measurement systems are presented. First, the measured data from both the systems are collected, then the data are processed to obtain the natural frequency and the mode shapes of the panel specimens. Subsequently, the ULS and the fitted modes using the GSM approach are calculated (see Section 2 for detail theory). Ultimately, the damage indices (see Eq. (10)) are calculated based on the

approaches described in Section 2. The feasibility and limitation of each system are evaluated and discussed as well.

6.2.1 SLV measurement system

The scanning laser vibrometer (SLV) system has the ability to measure small vibrations at a large number of points in relatively short time, and the mode shape obtained from the SLV system is the displacement one. The scanning processes are conducted using about 17×27 grids (459 points) for the healthy aluminum panel (Alu-CL-H) and 27×45 grids (1215 points) for the aluminum panel with saw-cut damage (Alu-CL-SD) (Figure 8(a)); while for the composite in clamped-clamped condition (Figure 8(b)), it is conducted using 12×17 grids (204 points). Example of the measurement grid for the aluminum panel (Alu-CL-H) is shown in Figure 12.
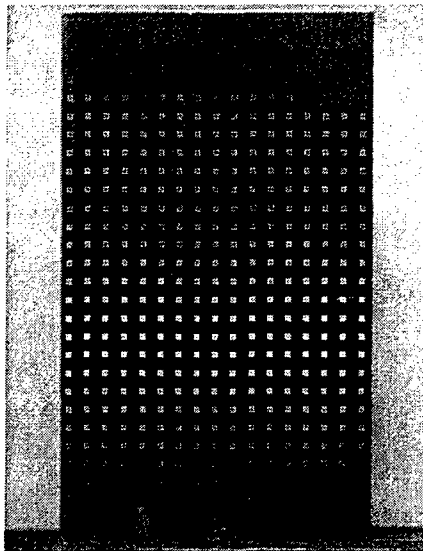

Figure 12 SLV scan grid points for aluminum panel (Alu-CL-H)

6.2.1.1 Natural frequencies and mode shapes data

The natural frequencies and mode shapes are obtained and presented in the following. For the aluminum panel, both the healthy (undamaged) and damaged data are available. For the composite panel with edge delamination, only data of damaged panel is available.

The measured frequencies for the panel specimens are presented in Tables 4 and 5. In the mode classification, the transverse bending modes in the cantilevered condition panel (i.e., the aluminum plate) are not exactly pure transverse but in the sense that the deflection shapes in the transverse direction are significantly dominant than the ones in other directions. The mixed modes mean that the effects of the deflections in the longitudinal and transverse directions are equally significant, and their forms combine deflection in both the directions. Examples of the mode shapes obtained from the SLV data are shown in Figure 13, i.e., the first six mode shapes of the composite panels with clamped-clamped boundary conditions (Comp-CC-ED).

Table 4 Experimental SLV frequencies of Aluminum panels, healthy (Alu-CL-H) and damaged (Alu-CL-SD)

Mode number	Healthy (Hz)	Damaged (Hz)	Type of mode
1	7.5	7.4	1st L-bending
2	29.5	29.2	1st T-bending
3	47.1	45.6	2nd L-bending
4	97.2	96.1	mixed
5	131.7	130	3rd L-bending
6	161.6	154.8	2nd T-bending
7	190.8	189.1	Mixed
8	228.4	224.7	Mixed
9	263	262	4th L-bending
10	321.4	319.4	Mixed
11	338.4	333.4	Mixed
12	413.9	394.7	3rd T-bending
13	433.8	432.3	5th L-bending
14	475.6	473. 3	Mixed
15	500	496.1	Mixed

Table 5 Experimental SLV frequencies of clamped-clamped composite panel with edge delamination (Comp-CC-ED)

Mode number	Frequency (Hz)	Type of mode
1	56.38	1st L-bending
2	61.25	Damage's mode
3	76.50	1st T-bending
4	160.5	2nd L-bending
5	189.7	Mixed
6	198.1	2nd T-bending
7	310	Mixed
8	330	3rd L-bending
9	363	Mixed
10	466.6	3rd T-bending
11	508.6	Damage's mode
12	568.3	Mixed
13	680.8	Mixed
14	715.2	Damage's mode
15	808.3	4th L-bending
16	887.7	4th T-bending
17	938	mixed

(a) First mode, 56.8 Hz

(b) Second mode, 76.5 Hz

(c) Third mode, 160.5 Hz

(d) Fourth mode, 189.7 Hz

(e) Fifth mode, 198.1 Hz

(f) Sixth mode, 310 Hz
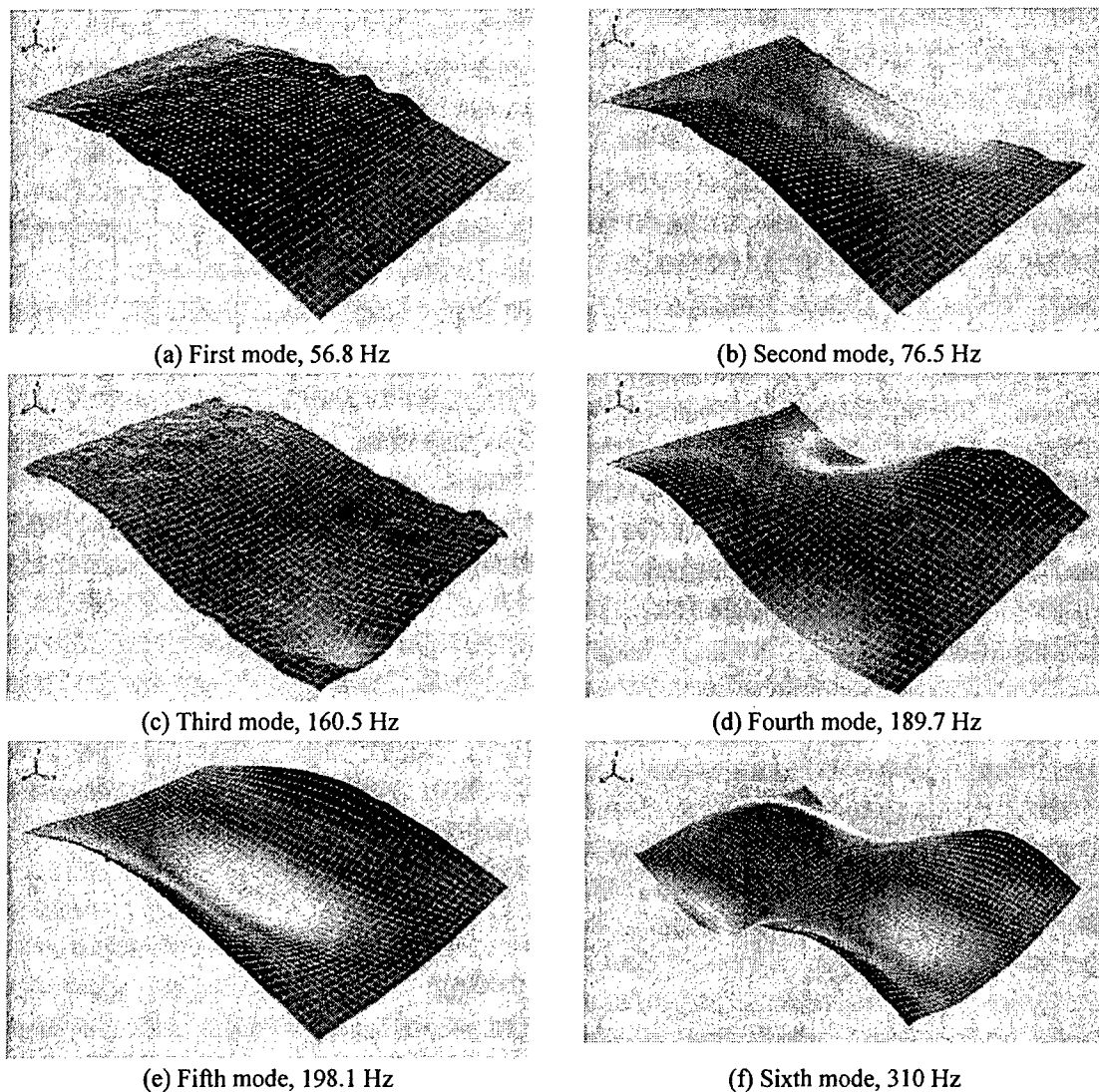
Figure 13 The first six mode shapes of the Comp-CC-ED panel from the SLV system

6.2.1.2 Damage identification

The uniform load surfaces and fitted mode shapes based on the gapped smoothing method are presented in the following figures. The purpose is to determine the ULS and the corresponding fitted mode shapes by using only a few low modes, since higher are more difficult to obtain (e.g., using the PVDF sensor system as introduced next). For the GSM curve-fitting processes, the polynomials in the order of four are sufficient for up to the sixth modes. In this study, the higher orders (i.e., up to the 8th order) of polynomial are used to fit the testing data and to improve the goodness of fit.

Depending on the orientation of the deflection modes, damage with certain orientation may have more significant effect on certain modes than others. Therefore, the ULS and fitted mode shapes are also calculated with different combination of mode shapes, representing different type

of modes, such as the transverse bending or longitudinal bending modes, to evaluate effect of damage orientation with respect to the mode direction.

Damage in the panel is identified by using the ULS and GSM (U_{GSM}) as introduced in Section 2. The Damage Index (Eq. (10)) and GFD (Eq. (2a)) distributions on the panel are calculated to identify the location of damages.

Aluminum panel with saw-cut (Alu-CL-SD)

The aluminum panel is tested in cantilever condition. The first measured mode shape has high noise inference. Hence, it is disregarded in the further calculations. The results of ULS and U_{GSM} calculation using five modes (2nd-6th modes) are presented in Figure 14, and the corresponding damage index is presented in Figure 15. The calculation based on the longitudinal bending mode shapes do not improve the identification result. However, the transverse bending mode shapes show much better result. Considering the damage effect on the first transverse bending is small, only the second and third transverse bending shapes are included in the calculation. The measured deflection ($U_{measured}$) and U_{GSM} calculated from the transverse bending modes are presented in Figures 16 and 17 for the second and the third mode, respectively. The corresponding damage index distributions are presented in Figure 18. The ULS and U_{GSM} calculated from both the transverse bending modes are presented in Figure 19, and the corresponding damage index distribution is presented in Figure 20. As shown in Figures 18 and 20, the location and relative magnitude of the damage (the saw-cut damage) are clearly illustrated.
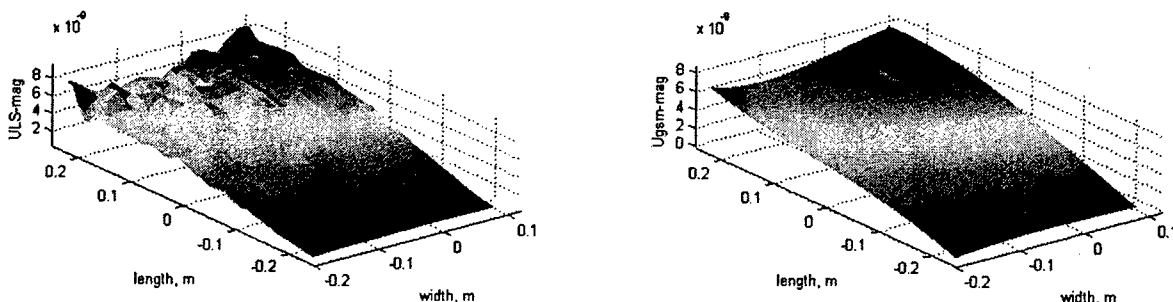

**Figure 14 The ULS and U_{GSM} of Alu-CL-SD using the first 5 mode shapes from the SLV system**
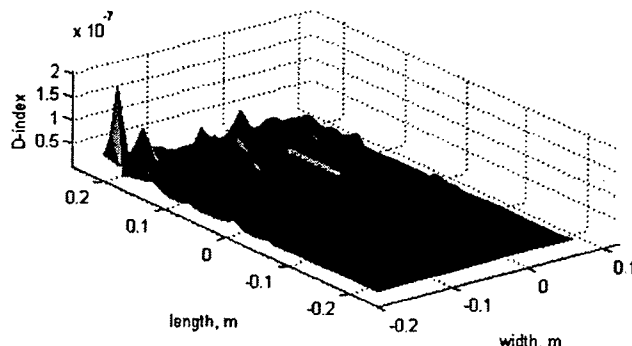
Figure 15 DI distribution of Alu-CL-SD using ULS from the first 5 mode shapes from the SLV system
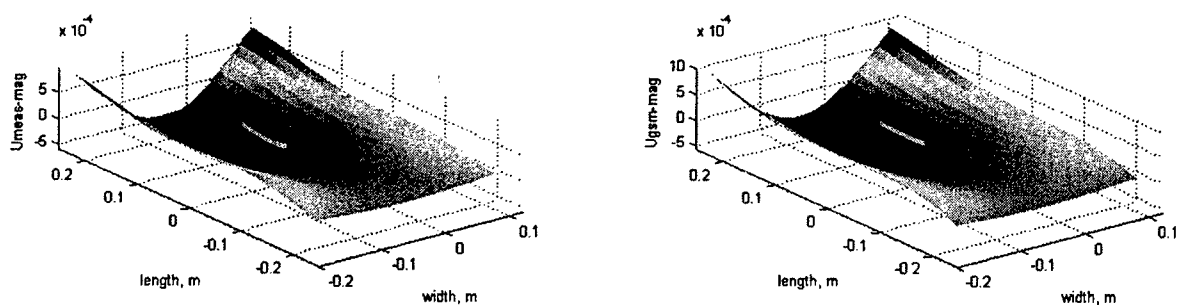
Figure 16 The $U_{measured}$ and U_{GSM} of Alu-CL-SD from the 2nd transverse bending mode shapes from the SLV system
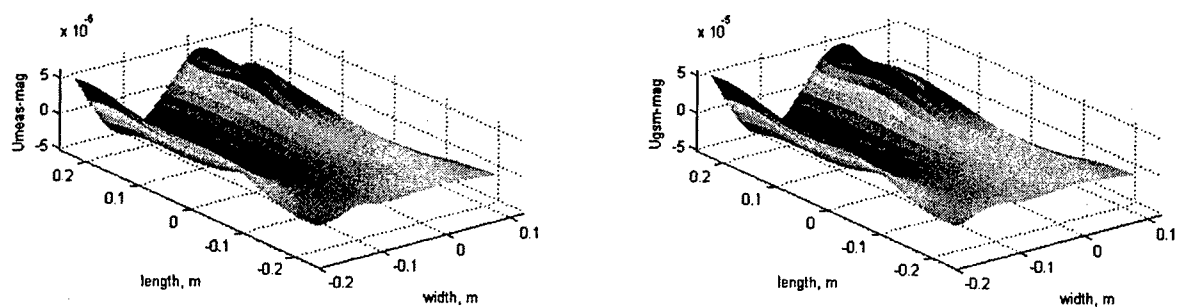

Figure 17 The $U_{measured}$ and U_{GSM} of Alu-CL-SD from the 3rd transverse bending mode shapes from the SLV system
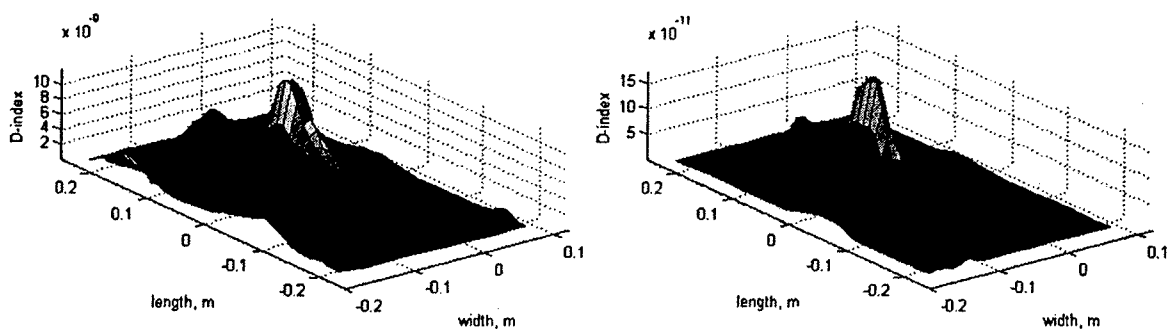
(a) 2nd transverse bending mode   (b) 3rd transverse bending mode

Figure 18 DI distribution of Alu-CL-SD from the transverse bending mode shapes from the SLV system
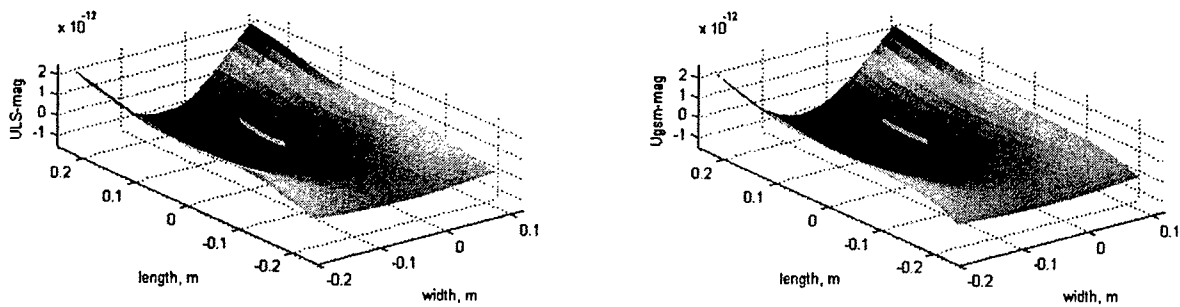
Figure 19 The ULS and U_{GSM} of Alu-CL-SD using the 2nd and 3rd transverse bending mode shapes from the SLV systems
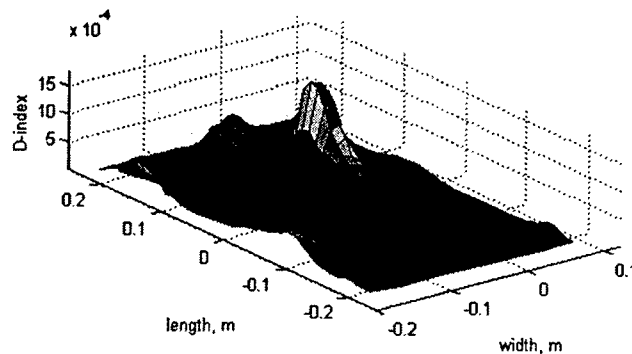

Figure 20 Damage Index distribution of Alu-CL-SD using ULS data from transverse bending mode shapes from the SLV system

Composite panel with edge delamination (Comp-CC-ED)

In this case, the composite panel is clamped at both ends, which later can be compared with the other approach that combines the static and dynamic loading. The first calculation is performed by using the first three mode shapes. The estimation for ULS and the U_{GSM} are presented in Figure 21, and the corresponding DI distribution over the panel using the first three mode shapes is presented in Figure 22(a). For comparison, the DI distribution calculated with the first five mode shapes is also presented in Figure 22(b). The results of the DI using the first three and five mode shapes are almost identical, thus validating that the proposed damage identification approach performs well by just using a few low mode shapes.

The next results are from the calculation performed with only using the first three transverse bending mode shapes. The ULS and the U_{GSM} are presented in Figure 23. These much higher mode shapes have low noise to signal ratio, which resulted in the much smoother damage index distribution other than in the location of damage, see Figure 24. Similar results are also obtained from the first three longitudinal bending mode shapes. The ULS and U_{GSM} are presented in Figure 25, and the damage index (DI) distribution is presented in Figure 26.
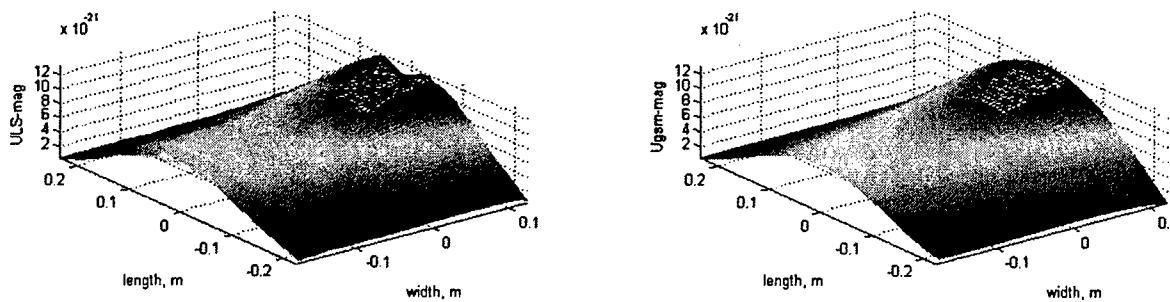
Figure 21 The ULS and U$_{GSM}$ of Comp-CC-ED using the first 3 mode shapes from the SLV system

(a) 3 mode shapes
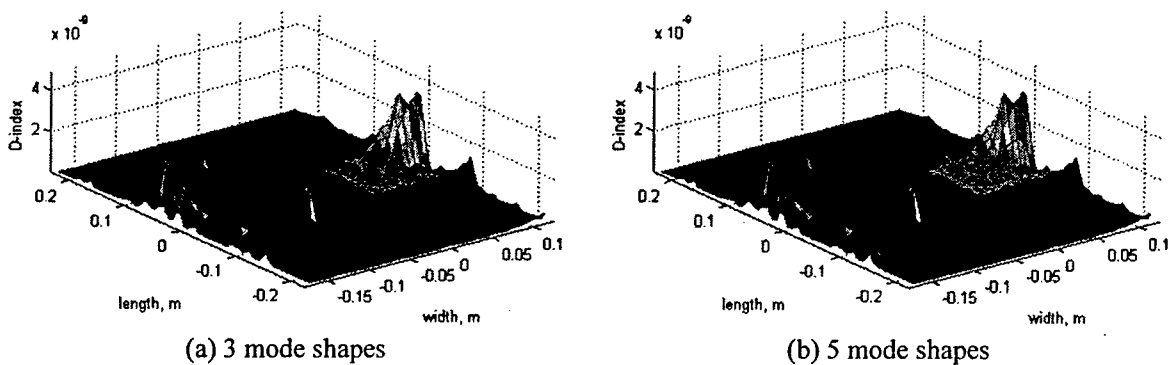
(b) 5 mode shapes

Figure 22 DI of Comp-CC-ED using ULS data of different mode shapes from the SLV system
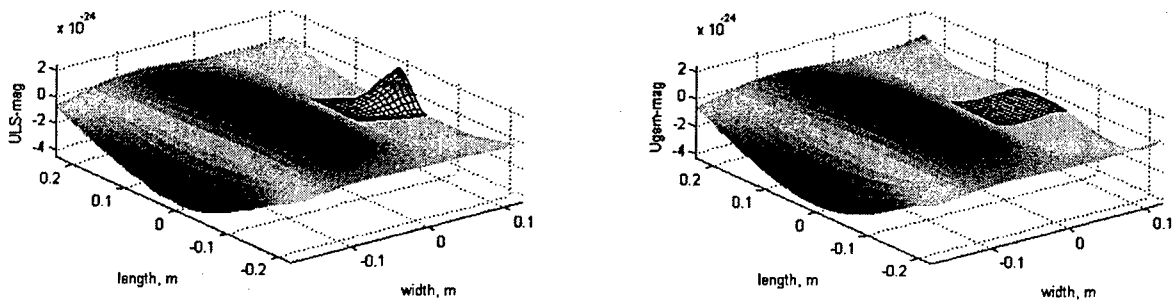
Figure 23 The ULS and U$_{GSM}$ of Comp-CC-ED using the 3 transverse bending mode shapes from the SLV system
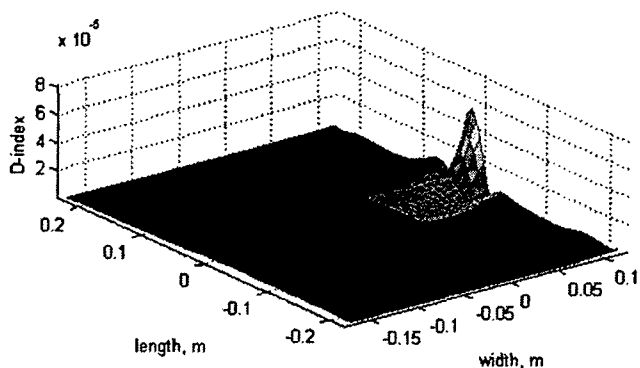
**Figure 24 DI distribution of Comp-CC-ED using ULS of the transverse bending mode shapes from the SLV system**
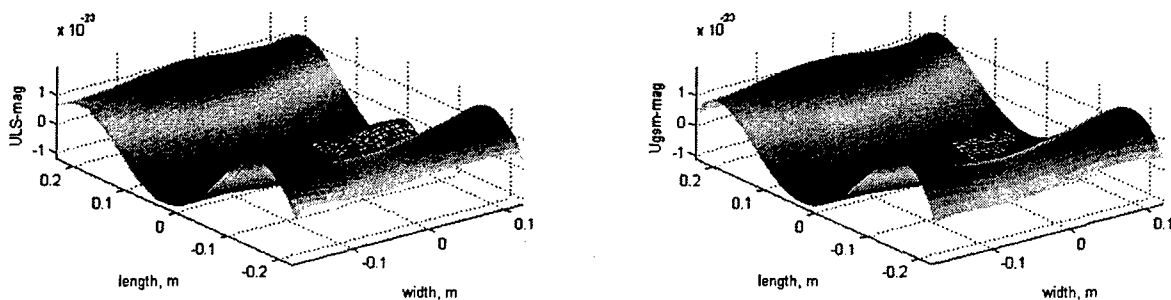
Figure 25 The ULS and U_{GSM} of Comp-CC-ED using the first 3 longitudinal bending mode shapes from the SLV system
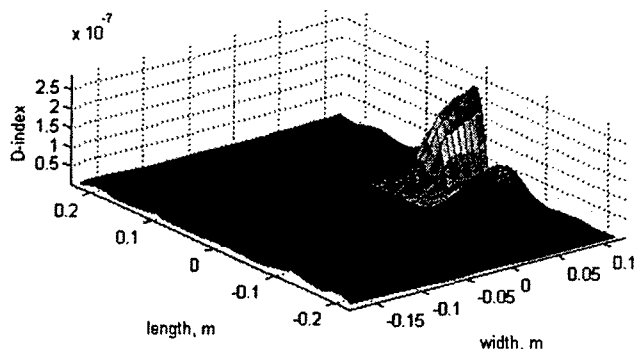

Figure 26 DI distribution of Comp-CC-ED using ULS of the longitudinal bending mode shapes from the SLV system

Damage identification based on the generalized fractal dimension (GFD) is also calculated for the Comp-CC-ED plate. The results from both the individual mode and the ULS are presented in Figure 27.

(a) 2nd mode	(b) ULS
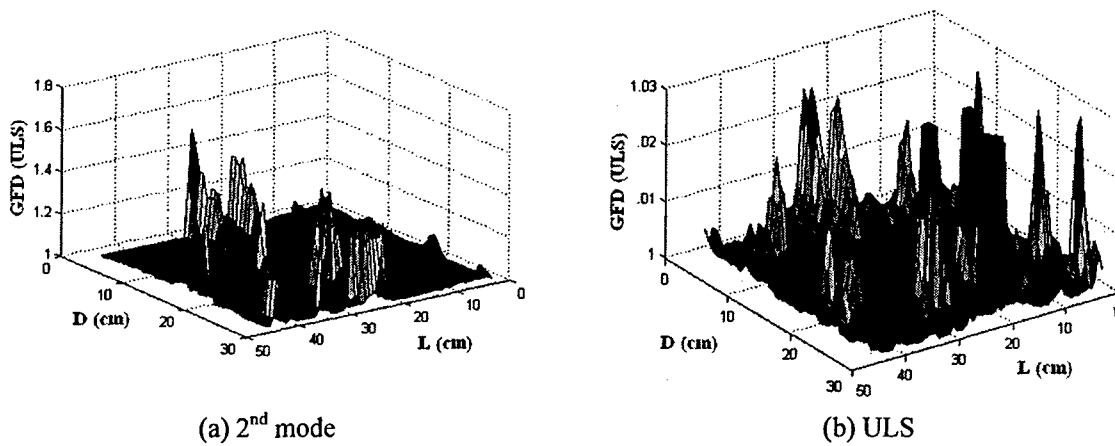
Figure 27 GFD results for Comp-CC-ED plate from the SLV data

6.2.2 PVDF sensor system

The measurement points in the PVDF sensor array experiment is much less than the one using scanning laser vibrometer (SLV). For the aluminum panel (Figure 8(a)) in the cantilever condition, the measurements are conducted using 12×18 grids (216 points); while for the composite in clamped-clamped condition (Figure 8 (b)), it is conducted using 12×17 grids (204 points).

6.2.2.1 Natural frequencies and mode shapes data

The measured natural frequencies of the three panels are presented in Tables 6 and 7. The noise and signal ratio at the low frequencies, i.e., the first and the second modes, from the cantilevered boundary, affects the mode shapes severely. These two mode shapes are disregarded for further calculation. Several mode shapes obtained by using MEscope are presented in Figure 28.

Table 6 Experimental PVDF frequencies of cantilever aluminum plates, Alu-CL-H and Alu-CL-SD

Mode number	Healthy (Hz)	Damaged (Hz)	Type of mode
1	7.51	7.12	1st L-bending
2	29.4	29	1st T-bending
3	46.9	46.1	2nd L-bending
4	96.5	95.4	2nd T-bending
5	131	129.	3rd L-bending
6	162	155.	Mixed
7	190	187	3rd T-bending
8	228	N/A	Mixed
9	262	260	4th L-bending
10	320	317	4th T-bending
11	338	333	Mixed
12	414	394	Mixed
13	433	430	5th L-bending
14	475	474	Mixed
15	498	494	5th T-bending

Table 7 Experimental PVDF Frequencies of cantilever composite panel with edge delamination, Comp-CC-ED

| Mode number	Healthy (Hz)	Type of mode
1	53.9	1st L-bending
2	63	Damage's mode
3	77.1	2nd L-bending
4	86.9	Damage's mode
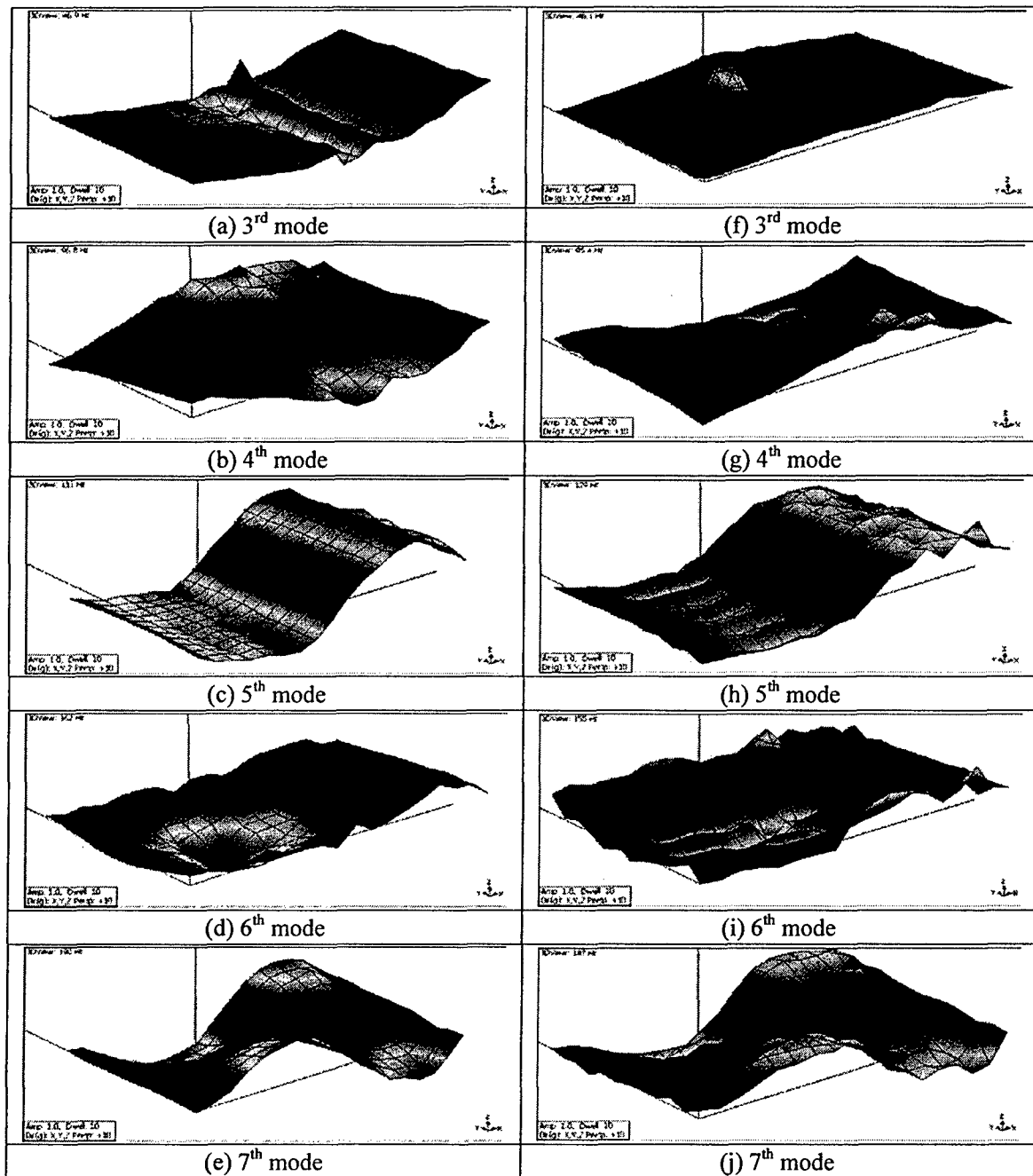
Figure 28 The curvature mode shapes of aluminum panels from the PVDF sensor system: (a-e) Alu-CL-H and (f-j) Alu-CL-SD

6.2.2.2 Damage identification

Similar to the SLV experiment, data from the PVDF sensor experiment are processed to obtain the ULS and U_{GSM} and ultimately to identify the damage. The results are reported in the following section.

Aluminum panel with saw-cut (Alu-CL-SD)

Figure 29 presents the ULS and U_{GSM} results of the aluminum panel using the first three mode shapes. The Damage Index (DI) distribution is presented in Figure 30. Results of ULS and U_{GSM} from transverse bending mode shapes (2nd and 3rd modes) are presented in Figure 31, and the corresponding Damage Index distribution is presented in Figure 32.
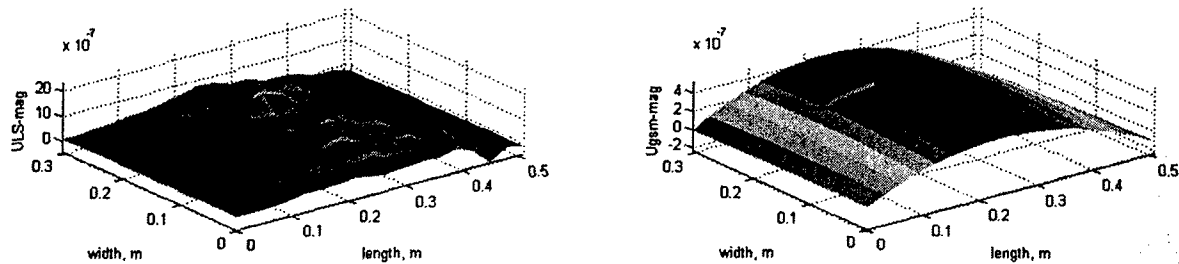

Figure 29 The ULS and U_{GSM} of Alu-CL-SD using the first 3 curvature mode shapes from the PVDF sensor system
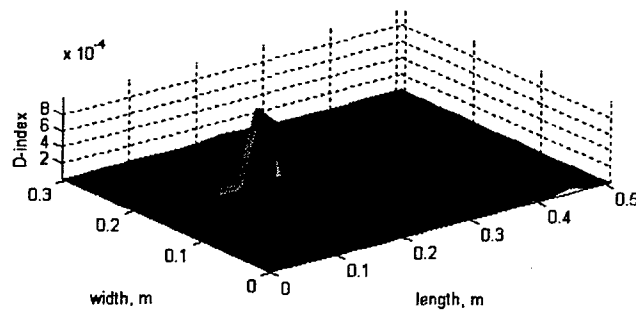

Figure 30 DI distribution of Alu-CL-SD using ULS from the first 3 curvature mode shapes from the PVDF sensor system
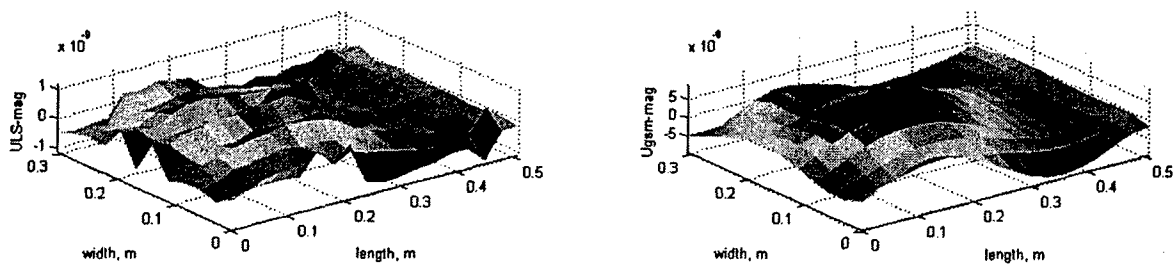

Figure 31 The ULS and U_{GSM} of Alu-CL-SD using the 2nd and 3rd transverse bending modes from the PVDF sensor system
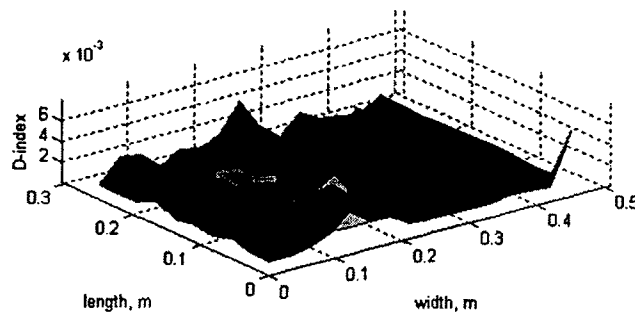
Figure 32 DI distribution of Alu-CL-SD using ULS from the transverse bending mode shapes from the PVDF sensor system

Composite panel with edge delamination (Comp-CC-ED)

The ULS and U_{GSM} results of the Comp-CC-ED panel using the first three mode shapes are presented in Figure 33, and the corresponding DI distribution is presented in Figure 34. Damage identification based on GFD is calculated as well, and the results are presented in the forms of both the individual mode and the ULS (see Figure 35). As shown in Figures 34 and 35, both the DI based on the GSM method and the GFD locates the edge delamination in the composite plate.
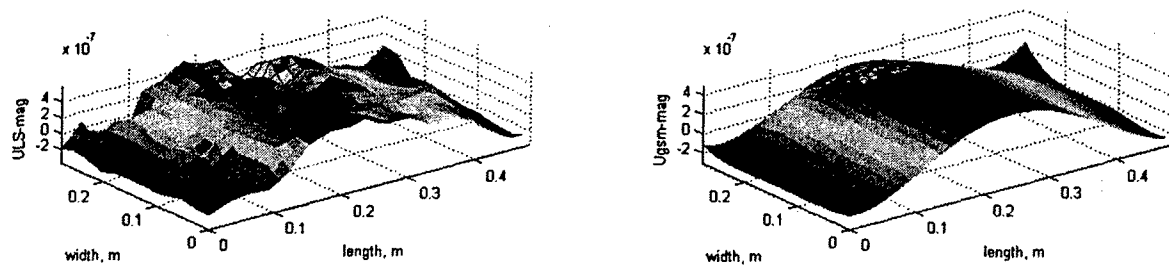

**Figure 33 The ULS and U_{GSM} of Comp-CC-ED using the first 3 curvature mode shapes from the PVDF sensor system**
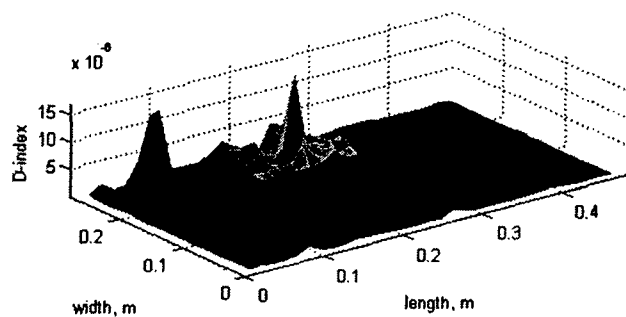
Figure 34 DI distribution of Comp-CC-ED using ULS from the first 3 curvature mode shapes from the PVDF sensor system

(a) 2nd mode   (b) ULS
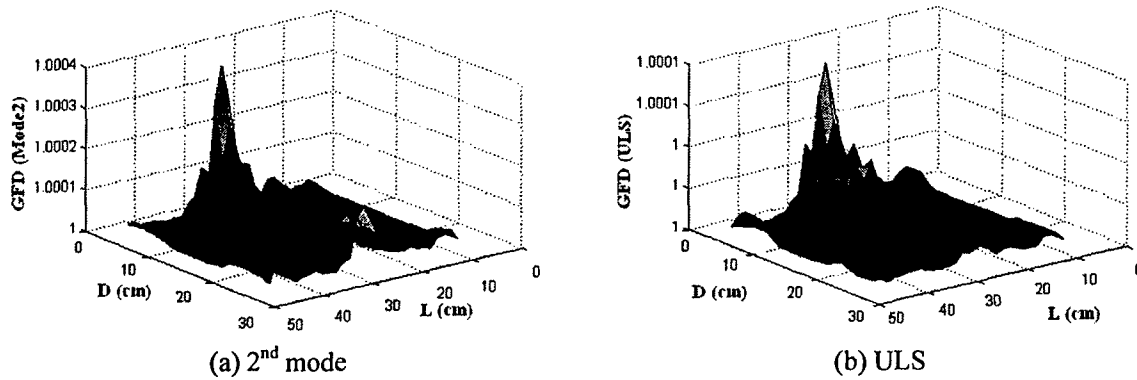
Figure 35 GFD results for Comp-CC-ED plate from the PVDF sensor data

6.2.3 Combined static/dynamic approach

The static/dynamic approach to enhance the damage detection is studied as well. The static loading is implemented by using a MTS machine (Figure 11), and testing with two compression loading cases (i.e., 600 lbs and 1,300 lbs) for the Comp-CC-ED plate is conducted. The dynamic testing combined with static loading increases the deflection of the specimens, which results in larger magnitude in damage identification. Results from the SLV data are presented in Figures 36 and 37, for the GSM and GFD approaches, respectively. Similarly, results from the GSM and GFD approaches using the PVDF sensor data are presented in Figures 38 and 39, respectively.
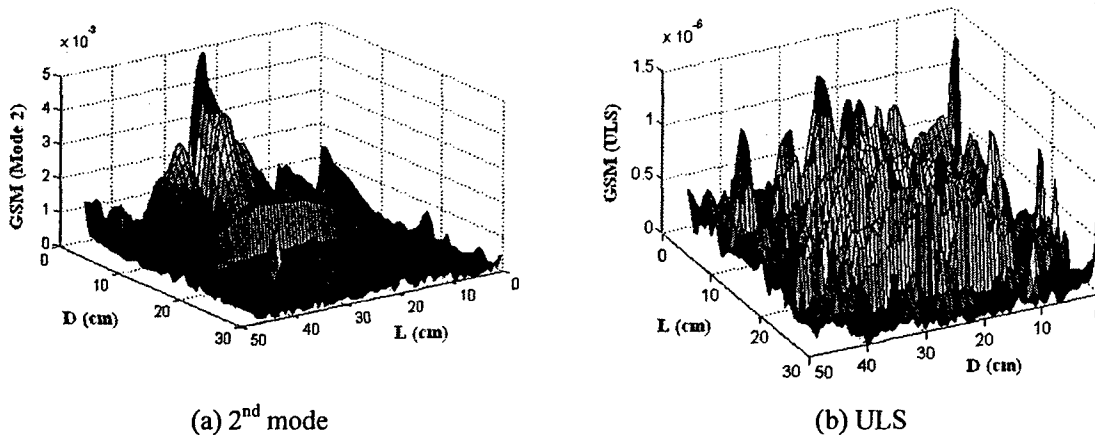
(a) 2nd mode   (b) ULS

Figure 36 Damage identification from GSM approach using static/dynamic loading ($P_c = 1,300$ lbs) from the SLV data.
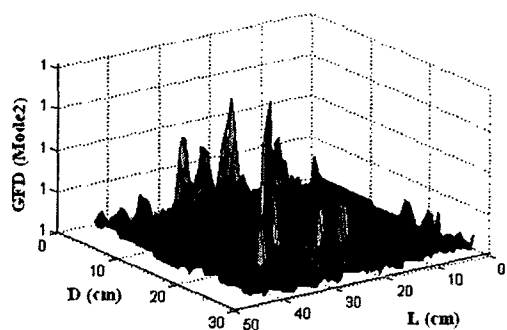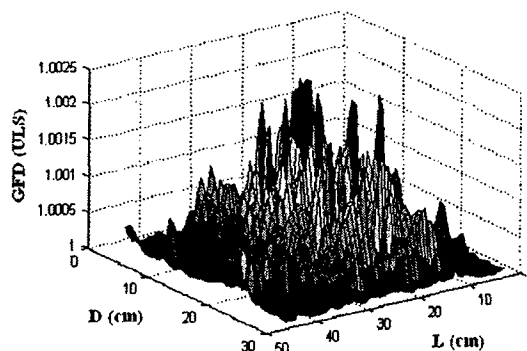
(a) 2nd mode

(b) ULS

Figure 37 Damage identification from GFD approach using static/dynamic loading (Pc = 1,300 lbs) from the SLV data.
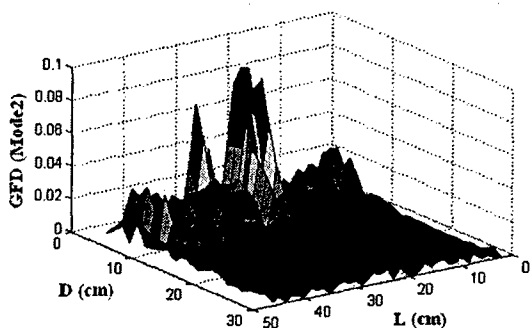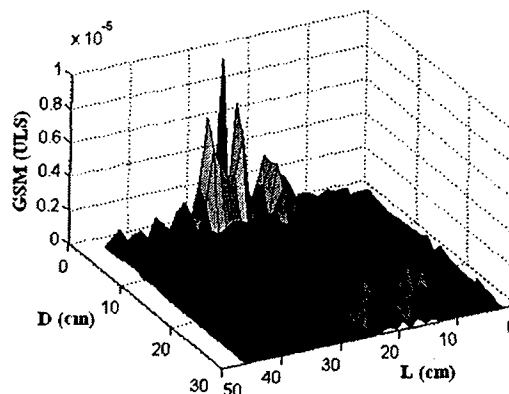
(a) 2nd mode

(b) ULS

Figure 38 Damage identification from GSM approach using static/dynamic loading (P_c = 1,300 lbs) from the PVDF sensor data.
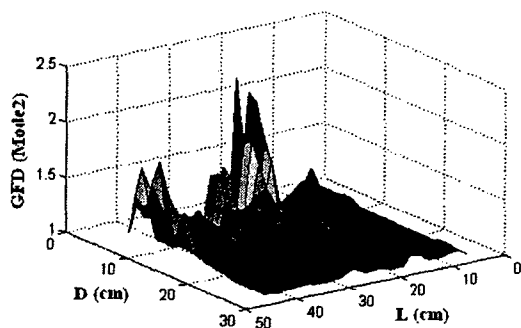
(a) 2nd mode
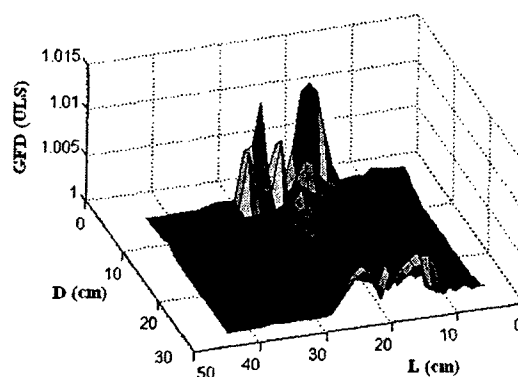
(b) ULS

**Figure 39 Damage identification from GFD approach using static/dynamic loading (P_c = 1,300 lbs) from the PVDF sensor data.**

6.3 Discussions

The results from the experimental demonstration show that the damage identification method based on the proposed approaches has properly identified two types of damage under studied, i.e., saw cut damage and edge delamination. The GSM approach works very well using low modes, where the mode shapes are properly estimated. Both the GSM and GFD approach work well without the baseline information from the healthy structures.

For the highly localized damage such as crack type of damage, which is simulated by a saw-cut damage in the demonstration, the damage has a significant effect on the mode shapes with the deformed direction perpendicular to the damage orientation. Therefore, damage identification using these mode shapes (e.g., the transverse ones for the longitudinal saw cut damage) yields better accuracy, see Section 6.2.1.2 and Figure 18. For the damage with relatively square dimension as in the case of composite plate with delamination, the orientation of the mode shapes with respect to the damage is hardly significant (see Comp-CC-ED results in Figures 22-25).

Although the PVDF sensor system is capable to identify the damage with a few low modes, the system needs careful attention regarding wiring system, sensor attachment method and proper shielding from interference, to obtain reliable measurement data. Integration of several PVDF sensors including the connection into an array in the form of large sheet may eliminate some of these concerns. Moreover, increase in the number of the measurement points will increase the accuracy and the number of mode shapes that can be acquired. However, the utilization of the ULS adapted in this study has improved the performance of the PVDF sensor system in damage detection.

The SLV system measuring the displacement mode shapes offers a non-contact measurement system without wiring and attachment problems. In general, the displacement mode shapes at low modes are insensitive to damage. However, the SLV system has the capability to obtain a large number of modes in relatively short time. Combined with the proposed damage identification approach, the SLV measurement system is a great tool for on-site damage monitoring system.

In this study, the location of the damage (e.g., the saw cut or delamination) is identified using both the SLV and PVDF sensor systems combined with the damage detection algorithms. The DI (using the GSM) and GFD plots can be also used in the static/dynamic tests to assess the relative magnitudes of the damage, and the further study on evaluating the magnitude of the respective damage is needed.

7 CONCLUSIONS

Several new findings and approaches in damage identification have been achieved in this STTR Phase I project, and they pave the foundation for further refinement of the dynamics-based method, implementation and potential product development. In particular, the following conclusions are reached:

(1) *SLV vs. PVDF measurement systems*: The damage detection algorithms using the displacement mode shapes measured from the SLV system and the curvature mode shapes directly measured from the PVDF sensors perform equally well in the identification procedure. But both the systems have their own unique advantages and disadvantages. The PVDF sensor has the potential to be integrated with the aircraft structures for on-board and real-time damage detection, thus increasing its

commercial viability through the integrated smart structural health monitoring (SHM) product development. However, the PVDF sensor system requires the wiring management since an array of the sensors is needed in dynamic mode shape measurement. The SLV has the advantage of eliminating the wiring and provides the non-contact and on-site measurement. Furthermore, the SLV system can acquire higher modes with less effort and be developed as a portable device for on-site implementation and monitoring.

(2) *ULS in improving the damage detection*: Application of uniform load surface (ULS) technique [9] show that the ULS converges very fast as the number of modes increases. Therefore, the ULS could be well approximated by the first few mode shapes. As demonstrated in this study, the ULS constructed from the first three-measured mode shapes proves to be adequate to identify damage in the aluminum and composite plates. Thus, the data processing considering the ULS improves the effectiveness of damage identification and can be used with other damage detection algorithms to evaluate the damage in the structures.

(3) *New damage detection algorithms*: The new damage detection algorithms – Generalized Fractal Dimension (GFD) and Damage Index (DI) using the Gapped Smoothing Method (GSM) recently developed by the investigators [8] are capable of identifying damage without baseline information from the original healthy structure. In particular, the location of the damage is clearly probed by the algorithms, and they have the potential for quantification of the damage by comparing the relative magnitude of the damage index. The effectiveness of the GFD and GSM approaches enhances the quality of damage identification, making the proposed dynamics-based method more effective and attractive for product development.

(4) *Static/dynamic approach*: Application of the combined static/dynamic loading increases the performance of the damage identification procedure. The comparisons of the structure with unloaded and loaded conditions demonstrate the purpose of the approach, i.e., probing the damage by enlarging the damage effect through applying the static loading. Development of a method to quantify the effectiveness of the static/dynamic approach is feasible using the static/dynamic approach.

(5) *Future Research:* Compilation of the processes in the identification procedure, especially in data processing, for further system integration is important in leading to the product development. A need exists to combine the new findings and improved techniques developed in this STTR Phase I project into an implementable, effective, and commercially-viable system for SHM of aircrafts, and it can be realized through the potential Phase II funding and other research opportunities. Good quality and reliable data are essential for the performance of the SHM system. The proposed approach using either the SLV or PVDF sensor system is effective in locating the damage, and future research is needed to quantify the damage and generate diagnostic or warning information for the structural status. The integration of the proposed SHM system with MEMS and wireless communication technologies leading to a viable product is worth exploring.

8 TECHNICAL FEASIBILITY

Complemented with programmable electronic devices or chips to process the data and the software system of computing the damage parameters developed in this study, the technology

based on the SLV measurement system has great potential for development of portable on-site monitoring system; while with development of sensor array system and wiring management scheme integrated with MEMS and wireless communication technologies, the technology using the PVDF sensor system is capable of performing on-board and real-time health monitoring. On the other hand, the promising sensor systems (e.g., PVDF) and damage detection algorithms (e.g., GFD and GSM) and schemes (e.g., ULS and combined static/dynamic technique) can be easily adopted by or integrated with other existing systems currently used in the field application.

As demonstrated in this Phase I project, the two sensor systems (SLV and PVDF) are readily applicable for damage detection and field implementation in SHM of aircrafts, and the damage detection algorithms and schemes developed, such as GFD and combined static/dynamic approach, can improve the effectiveness and quality of the systems for damage identification. The sensor systems and detection schemes are technically feasible and viable in implementation; however, the data analysis and processing may require the personnel with good understanding of dynamics and the techniques proposed in this study. A way to overcome this obstacle is by developing a user-friendly software and hardware package which integrates the sensor systems and damage detection schemes proposed in this study.

9 PARTICIPANTS AND PUBLICATIONS

Two principal investigators (Dr. Pizhong Qiao of ISSI and Dr. Wahyu Lestari of The University of Akron (UA)) have collaboratively involved in this research and conducted the proposed experimental and numerical study. Dr. Jialai Wang of the UA (now assistant professor at North Dakota State University) had contributed to this research and helped develop and mature the damage detection algorithms (i.e., generalized fractal dimension (GFD), gapped smoothing method (GSM), and uniformed load surface (ULS)) used in this study. He had involved in this STTR project between Aug 2004 and Dec 2005. In addition, two graduate students (Mr. Kan Lu and Ms. Mitali G. Shah) at UA have partially contributed to experimental and numerical work to this project.

The following publications are stemmed from this research effort:

1. Wang, JL and Qiao, PZ, "Improved Damage Detection of Beam-type Structures Using Uniform Load Surface," submitted to Structural Health Monitoring, Feb. 6, 2005.
2. Wang, JL and Qiao, PZ, "Development of Effective Damage Detection Algorithm for Beam-type Structures," 2005 Joint ASME/ASCE/SES Conference on Mechanics and Materials (McMat2005), Baton Rouge, LA, June 1-3, 2005. (6 pages)

The following publications resulted from this project have been in various stages of preparation, and they will be primarily submitted for journal review and possible publication by the investigators in the near future:

3. "Combined Static-dynamic Approach for Effective Damage Detection of Composite Plates," in preparation.
4. "Improved Damage Detection Algorithms for Plate-type Structures," in preparation.
5. "Damage Identification and Finite Element Analysis of Beam-type Structures," Finite Element in Analysis and Design, in preparation.
6. "Sensor Systems for Dynamics-based Structural Health Monitoring," Structural Health Monitoring, in preparation.

10 BIBLIOGRAPHY

[1] Chang, F.K., 1999, Structural health monitoring: a summary report, Proc 2nd International Workshop on Structural Health Monitoring.

[2] Doebling, S. W., Farrar, C. R., Prime, M. B., and Shevitz, D. W., 1996, Damage Identification and Health Monitoring of Structural and Mechanical Systems from Changes in Their Vibration Characteristics: A Literature Review, Report No. LA- I 3070-MS, Los Alamos National Laboratory.

[3] Paipetis SA, Dimarogonas, AD, Analytical methods in rotor dynamics. Elsevier Applied Science, London, 1986.

[4] Hamey CS, Lestari W, Qiao P., and Song G., Experimental damage identification of carbon/epoxy composite beams using curvature mode shapes. Structural Health Monitoring: An International Journal, in press.

[5] Kam TY, Lee TY. Detection of cracks in structures using modal test data. Engineering Fracture Mechanics 1992; 42, 381-387.

[6] Mandelbrot, B.B., 1967. How long is the coast of Britain? Statistical self-similarity and fractal dimension, Science, 156: 636-638.

[7] Hadjileontiadis, L.J., Douka, E., Trochidis, A., 2005. Fractal dimension analysis for crack identification in beam structures. Mechanical Systems and Signal Processing, 19, 659-674.

[8] Wang, J.L. and Qiao, P.Z., 2005, Damage detection and data processing using a generalized concept of fractal dimension, submitted to Structural Health Monitoring.

[9] Zhang, Z. and Aktan, A.E., 1998, Application of modal flexibility and its derivatives in structural identification, Research in Nondestructive Evaluation 10(1) 43-61.

[10] Ratcliffe, C.P. and Bagaria, A., 1998, A vibration technique for locating delamination in a composite beam, AIAA Journal 36(6) 1074-77.